Load Frequency Control Design for Complex Power Systems Implementing Integral Single-Phase Sliding Mode Control

Anh-Tuan Tran
Faculty of Electrical and Electronics Engineering, Ton Duc Thang University, Ho Chi Minh City, Vietnam
trananhtuan1@tdtu.edu.vn

Van Van Huynh
Modeling Evolutionary Algorithms Simulation and Artificial Intelligence, Faculty of Electrical and Electronics Engineering, Ton Duc Thang University, Ho Chi Minh City, Vietnam
huynhvanvan@tdtu.edu.vn (corresponding author)

Thinh Lam-The Tran
Faculty of Electrical and Electronics Engineering, Ton Duc Thang University, Ho Chi Minh City, Vietnam
42000133@student.tdtu.edu.vn

Received: 18 October 2024 | Revised: 27 November 2024 | Accepted: 1 December 2024

 DOI: https://doi.org/10.48084/etasr.9323

ABSTRACT

This paper proposes a Decentralized Integral Single-phase Sliding Mode Control (DISSMC) for Load Frequency Control (LFC) in Complex Power Systems with Multi-Source generation (CPSMS), integrating reheat, hydro, gas, and wind turbines. A generalized structure is employed to model Multi-Area Linked Power Systems (MALPS), providing a realistic representation of diverse power plants. The proposed method formulates an integral Sliding Surface (SS) to mitigate the chattering phenomena and ensures finite-time stability through a continuous control law. Additionally, a single-phase technique eliminates the reaching phase, ensuring immediate trajectory control. The MATLAB/Simulink simulations validate the DISSMC's effectiveness in stabilizing frequency fluctuations and managing load variations across three interconnected regions, each hosting different power plant types. The results highlight the proposed controller's robustness and adaptability to dynamic load and renewable energy source fluctuations.

Keywords-complex power system; load frequency control; sliding mode design

I. INTRODUCTION

Recently, there has been a huge development in power generating technology. Meanwhile, many countries are moving to reduce climate change by reducing their reliance on conventional power plants and replacing them with wind farms. This can be characterized by the sharp change in the amount of energy produced depending on wind speed, geographical location, etc. Moreover, there is an increase in the power demand and the load connected to the grid, which necessitates the creation of large power systems. Thus, there is a need to interconnect the different power plants, such as reheat plants, hydro power plants, gas plants, wind farms, etc. in order to meet the increasing energy demand. The interconnection of MALPS has made the LFC a very complex task due to the nonlinearity and system uncertainty [1]. The MALPS consists of a geographically dispersed power area. However, each area can be a linked multi-area or an isolated power plant. In this paper, the most general case according to which each area consists of multi-power sources is considered. The literature aims to ensure good power system performance through an effective control strategy. [2, 3]. The first control method used to monitor the frequency, and the output power of a single power plant was proportional-integral [4]. However, the PI controller works efficiently only when the power system operates near the nominal operating point. Otherwise, the former fails to stabilize the power flow or the frequency. Other control schemes, such as adaptive control [5], intelligent control [6], optimal control [7], and robust control [8, 9], have been studied, but they were designed for small, interconnected power grids and have not been proven effective for use in larger power systems. The Sliding Mode Control (SMC) is a robust control scheme, where the system is impervious to matched uncertainties and system disturbances [10]. Authors in

[11, 12] proposed the SMC to control the load frequency in single and multi-area power systems, respectively. The limitation of the multi-area system model in [12] was that it did not include different types of power plants as in a real-life system. Authors in [13] studied the nonlinear SMC for a multi-area power system. However, frequency chatter phenomena and discontinuous control signal are a major drawback of conventional SMC. Applying pure SMC in a practical system, causes wear and tear in the mechanical component, which leads to high power loss and reduces the efficiency of the power plant [14-17].

Integrating wind power into the conventional grid is a very challenging task due to the very wide fluctuations in the power generation from such renewable plants. Therefore, an adaptive control scheme is introduced to handle the continuous change of the operating point of such a large power system. The aforementioned LFC strategy can be only obtained when the following assumption is verified: the system aggregated uncertainties and disturbances are bounded by a known positive constant. However, this is not the case for a large power system including wind farms. Authors in [18] proposed an adaptive fuzzy controller to control a small hydropower plant. Authors in [19] used a genetic algorithm to optimize the integral control gain, which was utilized to train an adaptive network-based fuzzy inference system. Authors in [20] presented a load frequency controller-based indirect adaptive fuzzy technique for the interconnected power system. Also, authors in [21] studied a direct-indirect adaptive fuzzy controller, which was adapted in multi-area load frequency problems. The adaptive fuzzy techniques suffer from serious drawbacks, which can be seen in the large settling time and oscillations in the transient period. Authors in [22] proposed a decentralized adaptive SMC for multi-area power systems. The main contribution was the design of a SOISMC law that adopts the adaptive gain tuning. By applying this controller, the limitations in [23, 24], mainly the bounded uncertainties with a positive constant, are eliminated. Although the MALPS model is used, the different types of power plans are not considered. Authors in [25] introduced a chattering free adaptive SOISMC for a multi-area hydropower system, and authors in [26] studied the most general case of large power systems. Authors in [27] proposed an enhancement on the traditional SMC to ensure the convergence of all states to zero, where an additional supplementary controller-based Adaptive Dynamic Programming (ADP) was employed to enhance the ability of the controller to handle the fluctuation of the power system. The ADP succeeds in producing an adaptive control signal by changing the weight against the uncertainties and system parameters.

In this paper, the most general case of a multi-area linked power system containing renewable energy is considered. To the best of the authors' knowledge, no work has been reported in the LFC literature on the design of a robust SMC for such a realistic MALPS with a combination of thermal, hydro, gas, and wind generation units. In view of the above, the contributions of this paper can be stated as follows:

- The paper introduces a novel DISSMC tailored for LFC in CPSMS, including reheat, hydro, gas, and wind turbines.
- A generalized structure is proposed for modeling MALPS, enabling a more accurate and realistic representation of interconnected regions with diverse power plant types.
- The integral SS is designed to effectively eliminate chattering, while a single-phase technique removes the reaching time, ensuring faster and smoother trajectory convergence.
- MATLAB/Simulink simulations demonstrate the controller's capability to handle load variations and renewable energy source fluctuations across a CPSMS with three interconnected areas. The results confirm the robustness and adaptability of the proposed approach.

II. LFC ON CPSMS

In this section, the mathematical model of MALPS is presented. The power system under study consists of two geographically dispersed power areas. Area 1 was the largest area where five different types of power generation plants are aggregated together. Two plants were chosen to be a renewable power source. However, in both areas 2 and 3 there were no renewable plants and they are chosen to be topical to each other. The block diagram of such a MALPS can be illustrated as in Figure 1.

The proposed MALPS model consists of a reheat-turbine thermal power plant, a hydropower plant with a mechanical hydraulic governor, a gas turbine power plant, and a wind power plant. The system has 13 state variables and the associated vectors and matrices are:

$$x_i = [\Delta F_i \quad \Delta P_{m1i} \quad \Delta P_{Ri} \quad \Delta P_{SGi} \quad \Delta P_{m2i} \quad \Delta P_{RHi} \quad \Delta P_{GHi} \quad \Delta P_{m3i} \quad \Delta P_{Fi} \quad \Delta P_{Gi} \quad \Delta P_{GAi} \quad ACE \quad \Delta P_{tie,i}]^T$$

$$u_i = \left[\Delta P_{c1i} \quad \Delta P_{c2i} \quad \Delta P_{c3i}\right]^T$$

where the i^{th} area dynamic equations of MALPS are:

$$\Delta \dot{P}_{m1i} = \frac{-1}{T_{Ti}} \Delta P_{m1i} + \frac{1}{T_{Ti}} \Delta P_{Ri} \tag{1}$$

$$\Delta \dot{F}_i = -\frac{1}{T_{PSi}} \Delta F_i + \frac{K_{Psi}\alpha_{1i}}{T_{PSi}} \Delta P_{m1i} + \frac{K_{PSi}\alpha_{2i}}{T_{PSi}} \Delta P_{m2i} + \frac{K_{PSi}\alpha_{3i}}{T_{PSi}} \Delta P_{m3i} - \frac{K_{PSi}}{2\pi T_{PSi}} \sum_{i=1, j\neq i}^{N} K_{\text{ij}} \Delta P_{tiei} - \frac{K_{PSi}}{T_{PSi}} \Delta P_{di} \tag{2}$$

$$\Delta \dot{P}_{Ri} = \frac{-K_{Ri}}{T_{SGi} R_{1i}} \Delta F_i + \frac{-1}{T_{Ri}} \Delta P_{Ri} + \left(\frac{1}{T_{Ri}} - \frac{K_{Ri}}{T_{Sgi}}\right) \Delta P_{SGi} + \frac{K_{Ri}}{T_{SGi}} \Delta P_{c1i} \tag{3}$$

$$\Delta \dot{P}_{SGi} = \frac{-1}{T_{SGi} R_{1i}} \Delta F_i + \frac{-1}{T_{SGi}} \Delta P_{SGi} + \frac{1}{T_{SGi}} \Delta P_{c1i} \tag{4}$$

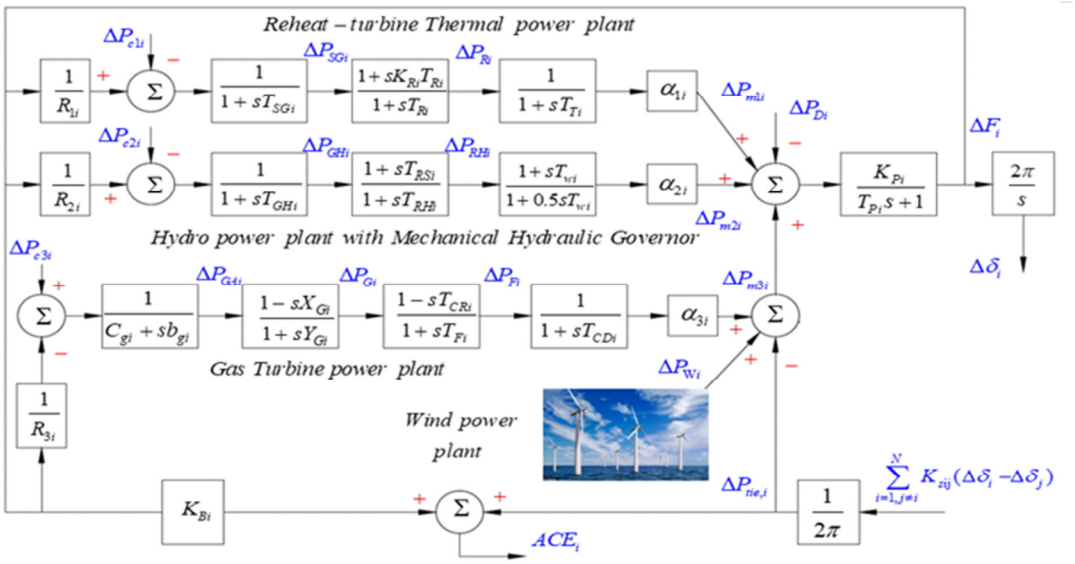

Fig. 1. The structure of the i[th] area LFC model in an MALPS.

$$\Delta\dot{P}_{m2i} = \frac{2T_{RSi}}{T_{RHi}T_{GHi}R_{2i}}\Delta F_i + \frac{-2}{T_{Wi}}\Delta P_{m2i} + (\frac{2}{T_{Wi}} + \frac{2}{T_{RHi}})\Delta P_{RHi} + (\frac{2T_{RSi}}{T_{RHi}T_{GHi}} - \frac{2}{T_{RHi}})\Delta P_{GHi} + \frac{-2T_{RSi}}{T_{RHi}T_{GHi}}\Delta P_{c2i} \quad (5)$$

$$\Delta\dot{P}_{RHi} = \frac{-T_{RSi}}{T_{RHi}T_{GHi}R_{2i}}\Delta F_i + (\frac{1}{T_{RHi}} - \frac{T_{RSi}}{T_{RHi}T_{GHi}})\Delta P_{GHi} + \frac{T_{RSi}}{T_{RHi}T_{GHi}}\Delta P_{c2i} + \frac{-1}{T_{RHi}}\Delta P_{RHi} \quad (6)$$

$$\Delta\dot{P}_{GHi} = \frac{-1}{T_{GHi}R_{2i}}\Delta F_i + \frac{-1}{T_{GHi}}\Delta P_{GHi} + \frac{1}{T_{GHi}}\Delta P_{c2i} \quad (7)$$

$$\Delta\dot{P}_{m3i} = \frac{-1}{T_{CDi}}\Delta P_{m3i} + \frac{1}{T_{CDi}}\Delta P_{Fi} \quad (8)$$

$$\Delta\dot{P}_{Fi} = \frac{T_{CRi}X_{Gi}}{T_{Fi}R_{3i}Y_{Gi}b_{gi}}\Delta F_i + \frac{-1}{T_{Fi}}\Delta P_{Fi} + (\frac{1}{T_{Fi}} + \frac{T_{CRi}}{T_{Fi}Y_{Gi}})\Delta P_{Gi} + (\frac{T_{CRi}X_{Gi}c_{gi}}{T_{Fi}Y_{Gi}b_{gi}} - \frac{T_{CRi}}{T_{Fi}Y_{Gi}})\Delta P_{GAi} - \frac{X_{Gi}T_{CRi}}{T_{Fi}Y_{Gi}b_{gi}}\Delta P_{c3i} \quad (9)$$

$$\Delta\dot{P}_{Gi} = \frac{-X_{Gi}}{R_{3i}Y_{Gi}b_{gi}}\Delta F_i + \frac{-1}{Y_{Gi}}\Delta P_{Gi} + (\frac{1}{Y_{Gi}} - \frac{Y_{Gi}c_{gi}}{Y_{Gi}b_{gi}})\Delta P_{GAi} + \frac{X_{Gi}}{Y_{Gi}b_{gi}}\Delta P_{c3i} \quad (10)$$

$$\Delta\dot{P}_{GAi} = \frac{-1}{R_{3i}b_{gi}}\Delta F_i + \frac{-c_{gi}}{b_{gi}}\Delta P_{GAi} + \frac{1}{b_{gi}}\Delta P_{c3i} \quad (11)$$

$$A\dot{C}E_i = K_{Bi}K_{Ei}\Delta F_i + \frac{K_{Ei}}{2\pi}\sum_{i=1,\,j\neq i}^{N} K_{ij}\Delta P_{tiei} \quad (12)$$

$$\Delta\dot{P}_{tiei} = 2\pi T_{ij}(\Delta F_i - \Delta F_j) \quad (13)$$

The system modeling of the i^{th} area is given by:

$$\dot{x}_i(t) = A_i x_i(t) + B_i u_i(t) + \sum_{j=1,\,j\neq i}^{N} H_{ij}x_j(t) + F_i\Delta P_{di}(t) \quad (14)$$

where $x_i(t) \in R^n$ represents the state vector, $u_i(t) \in R^m$ is the control vector, A_i, B_i, F_i, H_{ij} are the constant matrix equivalent i^{th} of each area $\left(A_i \in R^{n\times n}, B_i \in R^{n\times n}, F_i \in R^{n\times n}\right)$, and ΔP_{di} is the load disturbance.

Assumption 1. The load disturbance is assumed to be bounded and satisfy the following condition:

$$\left\|\Delta P_{di}\right\| < \partial_i, \quad i = 0,\ 1,\ 2,\ ...,\ N \quad (15)$$

where ∂_i is the unknown positive constant.

III. NEW SMC STRUCTURE

A. Integral single-phase SS

This section emphasizes the initial phase of suggesting a comprehensive SS for the MALPS. The integral single-phase SS is given as:

$$\vartheta_i(t) = \varsigma_i x_i(t) - \int_0^t \varsigma_i K_{mat}\, x_i(\tau)d\tau - \varsigma_i x_i(0)e^{-\alpha_i t} \quad (16)$$

where ς_i and ℓ_i are the constant matrix and the design matrix, respectively. Matrix ς_i is selected to make sure that matrix $\varsigma_i B_i$ is non-singular. The matrix $\ell_i \in R^{m_i \times n_i}$ is selected to meet the inequality.

$$\mathrm{Re}[\lambda_{\max}(A_i - B_i \ell_i)] < 0 \tag{17}$$

Deriving $\vartheta_i(t)$ gives:

$$\begin{aligned}\dot{\vartheta}_i(t) = {} & \varsigma_i A_i x_i(t) + \varsigma_i B_i u_i(t) + \sum_{\substack{j=1 \\ j \neq i}}^{N} \varsigma_i H_{ij} x_j(t) + \varsigma_i F_i \Delta P_{di} \\ & - \varsigma_i K_{mat} x_i(t) + \alpha_i \varsigma_i x_i(0) e^{-\alpha_i t}\end{aligned} \tag{18}$$

where $K_{mat} = (A_i - B_i \ell_i)$.

Setting $\dot{\vartheta}_i(t) = \vartheta_i(t) = 0$, the equivalent control is derived:

$$\begin{aligned}u_i^{eq}(t) = {} & -(\varsigma_i B_i)^{-1} [\varsigma_i B_i \ell_i x_i(t) + \varsigma_i F_i \Delta P_{di} + \alpha_i \varsigma_i x_i(0) e^{-\alpha_i t} \\ & + \sum_{\substack{j=1 \\ j \neq i}}^{N} \varsigma_i H_{ij} x_j(t)]\end{aligned} \tag{19}$$

B. Control System Design

The controller signal for the MAPS can be described as:

$$u_i(t) = u_i^r(t) + u_i^{sw}(t) \tag{20}$$

where:

$$\begin{aligned}u_i^r(t) = {} & -(\varsigma_i B_i)^{-1} [\varsigma_i B_i \ell_i x_i(t) + \sum_{\substack{j=1 \\ j \neq i}}^{N} \varsigma_i H_{ij} x_j(t) \\ & + \alpha_i \varsigma_i x_i(0) e^{-\alpha_i t}]\end{aligned} \tag{21}$$

and:

$$u_i^{sw}(t) = -(\varsigma_i B_i)^{-1} \delta_i \, sat[\vartheta_i(t)] \tag{22}$$

where δ_i is a non-negative constant and:

$$sat[\vartheta_i(t)] = \begin{cases} sgn[\vartheta_i(t)], \; if \; |S_i(\vartheta_i)| > \rho_i \\ \vartheta_i / \rho_i \quad , otherwise \end{cases} \tag{23}$$

Theorem 1: For the closed loop MALPS (14) and controller (20), every trajectory is directed towards the SS $\vartheta_i(t) = 0$ and once the trajectory is on the SS $\vartheta_i(t) = 0$ it remains thereafter.

Proof: A Lyapunov function is selected as:

$$\bar{V}(t) = \sum_{i=1}^{N} \left[\left\| \vartheta_i(t) \right\| \right] \tag{24}$$

The derivative of $\bar{V}(t)$ yields:

$$\dot{\bar{V}} = \sum_{i=1}^{N} \frac{\vartheta_i^T(\vartheta)}{\left\| \vartheta_i(\vartheta) \right\|} \{\dot{\vartheta}_i(t)\} \tag{25}$$

Substituting (18) into (25) gives:

$$\begin{aligned}\dot{\bar{V}} = {} & \sum_{i=1}^{N} \frac{\vartheta_i^T(\vartheta)}{\left\| \vartheta_i(\vartheta) \right\|} \{\varsigma_i A_i x_i(t) + \varsigma_i B_i u_i(t) + \sum_{\substack{j=1 \\ j \neq i}}^{N} \varsigma_i H_{ij} x_j(t) \\ & + \varsigma_i F_i \Delta P_{di} - \varsigma_i (A_i - B_i \ell_i) x_i(t) + \alpha_i \varsigma_i x_i(0) e^{-\alpha_i t}\}\end{aligned} \tag{26}$$

Using (20) and (26) we achieve:

$$\dot{\bar{V}}(t) \leq -\sum_{i=1}^{N} \delta_i \left\| \vartheta_i(t) \right\| \tag{27}$$

The above inequality implies that the state trajectories of the MALPS (14) reach the SS $\vartheta_i(t) = 0$ and stay on it thereafter.

IV. CASE STUDY AND RESULTS

In this section, simulations have been performed to demonstrate the feasibility and effectiveness of the proposed controller. For this purpose, two different setups were investigated:

- Scenario 1: The step load change is applied to the conventional MALPS without renewable plants, where the nominal parameter was used in all plants.
- Scenario 2: Exhibit the robustness of the proposed controller under the effect of renewable energy sources.

A. Scenario 1: Without renewable plants

In this base case, the nominal parameters of the MALPS are used. Let the value of the step load disturbance in each area be selected as $0.05(MW\ p.u)$ at time *t*=0 s. As can be seen in Figure 2, the controller achieved a faster response as the settling time of the frequencies in all three areas was 5 seconds, whereas it was slightly higher for the controller in [25]. Moreover, there were no chattering phenomena after reaching the steady state period. Table I covers the refinement of the system performance when implementing the proposed controller.

Figure 2 shows the frequency deviation of the three areas when load disturbance is introduced. Figures 3-5 depict the mechanical power for each power plant in the three areas. It is worth noting that in all systems, the signals are driven to zero at a faster settling time and small over/undershoot. Figure 6 illustrates the tie-line power deviation of the three areas and Table I presents the comparison of the results.

TABLE I. COMPARISON OF THE PROPOSED CONTROLLER WITH THE CONTROLLER IN [25]

Methods	**Proposed**		**[25]**	
Parameters	T_s	***M.O. S***	T_s	***M.O. S***
Δf_1	7.0	0.038	7.5	-0.17
Δf_2	7.0	0.032	7.5	-0.06
Δf_3	7.0	0.032	7.5	

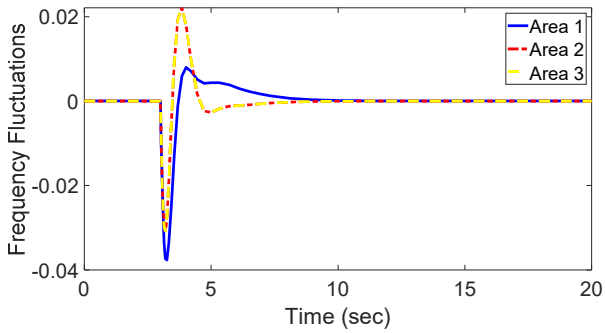

Fig. 2. The frequency deviations under scenario 1.

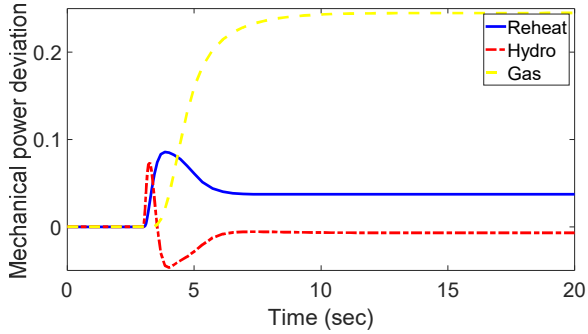

Fig. 3. Mechanical power deviation of area 1 under scenario 1.

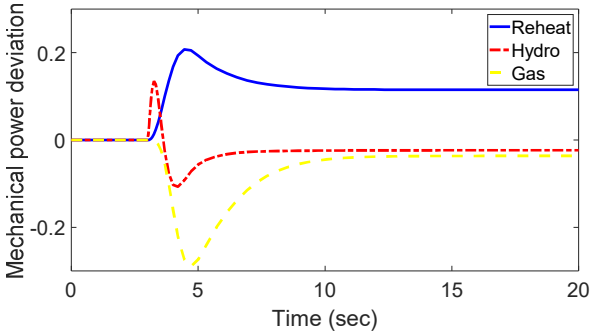

Fig. 4. Mechanical power deviation of area 2 under scenario 1.

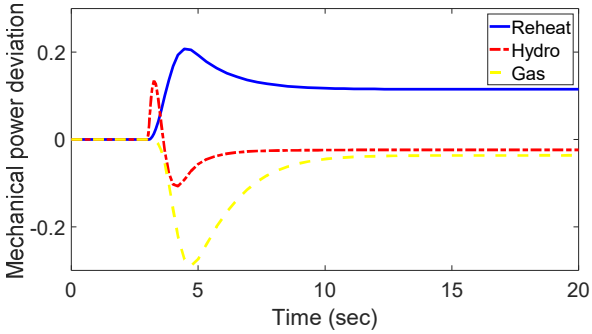

Fig. 5. Mechanical power deviation of area 3 under scenario 1.

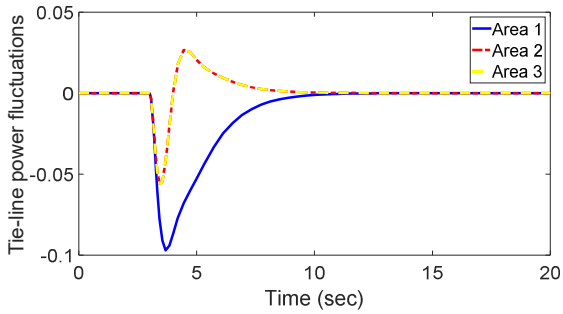

Fig. 6. Tie-line power deviation under scenario 1.

Remark 1: The proposed controller, utilizing DISSMC, outperforms the controller designed in [25] by achieving faster settling times and lower overshoot. This demonstrates its superior ability to efficiently stabilize the system while minimizing transient oscillations, thus ensuring a robust and reliable LFC even under CPSMS conditions.

B. Scenario 2: With renewable plants

In this case, the nominal parameters of the MALPS are used. The load disturbances for areas 1, 2, and 3 are assumed to be a 1%, 1.5%, and a 2% load change at t=3 s, respectively. Moreover, the impact of the renewable energy in the first area on the change of frequency is considered. Figures 7 and 8 display the frequency and tie-line power changes under scenario 2, respectively. The performance of the proposed approach is assessed to combat the load demand and wind speed changes. It also exhibits effectiveness in large MALPS for over/undershoots and defined time, with minimal impact.

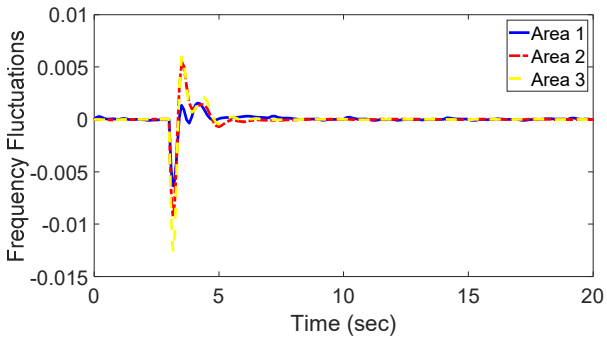

Fig. 7. The frequency deviations under scenario 2.

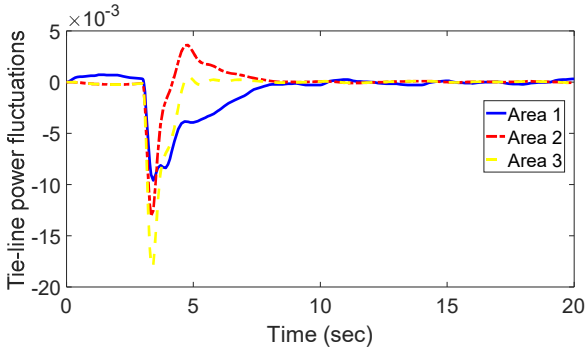

Fig. 8. Tie-line power deviation under scenario 2.

Remark 2: The proposed controller demonstrates exceptional capability in managing the variability and uncertainty introduced by renewable energy sources, such as wind turbines. By effectively mitigating frequency deviations and ensuring quick stabilization, the controller showcases its robustness and adaptability, making it a superior solution for integrating renewable plants into CPSMS.

V. CONCLUSION

In this paper, a Decentralized Integral Single-phase Sliding Mode Control (DISSMC) is designed and tested for a Multi-Area Linked Power System (MALPS). The most general case for a large power system containing five different types of renewable and conventional power plants has been modeled and controlled via a decentralized control approach. The challenges of integrating a renewable energy system with a conventional system, mainly the constant fluctuation of the output power and the unknown upper bound, have been solved by using a robust control scheme and an optimal Sliding Surface (SS) design has been achieved. The simulations demonstrate the feasibility and robustness of the proposed controller, which was evident from the system performance and the elimination of chattering phenomena. Fast recovery and less overshoot were observed when load disturbances were applied to the system.

ACKNOWLEDGMENT

This research is funded by Ton Duc Thang University under grant number <FOSTECT.2023.30>.

REFERENCES

[1] P. M. Anderson and A. A. Fouad, *Power System Control and Stability*, 1st ed. Piscataway, NJ, USA: Wiley-IEEE Press, 1993.

[2] M. Wadi, A. Shobole, W. Elmasry, and I. Kucuk, "Load frequency control in smart grids: A review of recent developments," *Renewable and Sustainable Energy Reviews*, vol. 189, Jan. 2024, Art. no. 114013, https://doi.org/10.1016/j.rser.2023.114013.

[3] R. Verma, S. K. Gawre, N. P. Patidar, and S. Nandanwar, "A state of art review on the opportunities in automatic generation control of hybrid power system," *Electric Power Systems Research*, vol. 226, Jan. 2024, Art. no. 109945, https://doi.org/10.1016/j.epsr.2023.109945.

[4] E. Çelik, "Exponential PID controller for effective load frequency regulation of electric power systems," *ISA Transactions*, vol. 153, pp. 364–383, Oct. 2024, https://doi.org/10.1016/j.isatra.2024.07.038.

[5] M. A. Abdel Ghany, M. A. Mosa, A. M. Abdel Ghany, and M. Y. Yousef, "Improving the frequency response of a multi-generation power system using adaptive variable structure fuzzy controller," *Electric Power Systems Research*, vol. 232, Jul. 2024, Art. no. 110368, https://doi.org/10.1016/j.epsr.2024.110368.

[6] Z. Li, J. Gao, and Y. Yang, "Provisional Microgrid Frequency Regulation by Brain Emotional Learning Based Intelligent Controller and Implementation Through FPGA," *Journal of Electrical Engineering & Technology*, vol. 19, no. 3, pp. 1217–1226, Mar. 2024, https://doi.org/10.1007/s42835-023-01656-z.

[7] N. Hasan, Ibraheem, and P. Kumar, "Optimal Automatic Generation Control of Interconnected Power System Considering New Structures of Matrix Q," *Electric Power Components and Systems*, vol. 41, no. 2, pp. 136–156, Jan. 2013, https://doi.org/10.1080/15325008.2012.732661.

[8] M. R. Toulabi, M. Shiroei, and A. M. Ranjbar, "Robust analysis and design of power system load frequency control using the Kharitonov's theorem," *International Journal of Electrical Power & Energy Systems*, vol. 55, pp. 51–58, Feb. 2014, https://doi.org/10.1016/j.ijepes.2013.08.014.

[9] V. V. Huynh, B. L. N. Minh, E. N. Amaefule, A.-T. Tran, and P. T. Tran, "Highly Robust Observer Sliding Mode Based Frequency Control for Multi Area Power Systems with Renewable Power Plants," *Electronics*, vol. 10, no. 3, Jan. 2021, Art. no. 274, https://doi.org/10.3390/electronics10030274.

[10] D. W. Qian, X. J. Liu, and J. Q. Yi, "Robust sliding mode control for a class of underactuated systems with mismatched uncertainties," *Proceedings of the Institution of Mechanical Engineers, Part I: Journal of Systems and Control Engineering*, vol. 223, no. 6, pp. 785–795, Sep. 2009, https://doi.org/10.1243/09596518JSCE734.

[11] A. T. Tran, N. T. Pham, V. Van Huynh, and D. N. M. Dang, "Stabilizing and Enhancing Frequency Control of Power System Using Decentralized Observer-Based Sliding Mode Control," *Journal of Control, Automation and Electrical Systems*, vol. 34, no. 3, pp. 541–553, Jun. 2023, https://doi.org/10.1007/s40313-022-00979-y.

[12] V. V. Huynh *et al.*, "Load Frequency Control for Multi-Area Power Plants with Integrated Wind Resources," *Applied Sciences*, vol. 11, no. 7, Apr. 2021, Art. no. 3051, https://doi.org/10.3390/app11073051.

[13] S. Prasad, S. Purwar, and N. Kishor, "Non-linear sliding mode load frequency control in multi-area power system," *Control Engineering Practice*, vol. 61, pp. 81–92, Apr. 2017, https://doi.org/10.1016/j.conengprac.2017.02.001.

[14] N. K. Nguyen, D. T. Nguyen, and T. M. P. Dao, "A Novel PSO-Based Modified SMC for Designing Robust Load-Frequency Control Strategies," *Engineering, Technology & Applied Science Research*, vol. 13, no. 4, pp. 11112–11118, Aug. 2023, https://doi.org/10.48084/etasr.5972.

[15] H. H. Alhelou, N. Nagpal, N. Kassarwani, and P. Siano, "Decentralized Optimized Integral Sliding Mode-Based Load Frequency Control for Interconnected Multi-Area Power Systems," *IEEE Access*, vol. 11, pp. 32296–32307, 2023, https://doi.org/10.1109/ACCESS.2023.3262790.

[16] A. T. Tran, M. P. Duong, N. T. Pham, and J. W. Shim, "Enhanced sliding mode controller design via meta-heuristic algorithm for robust and stable load frequency control in multi-area power systems," *IET Generation, Transmission & Distribution*, vol. 18, no. 3, pp. 460–478, Feb. 2024, https://doi.org/10.1049/gtd2.13077.

[17] J. Xia and H. Ouyang, "Chattering Free Sliding-Mode Controller Design for Underactuated Tower Cranes With Uncertain Disturbance," *IEEE Transactions on Industrial Electronics*, vol. 71, no. 5, pp. 4963–4975, May 2024, https://doi.org/10.1109/TIE.2023.3281665.

[18] D. V. Doan, K. Nguyen, and Q. V. Thai, "Load-Frequency Control of Three-Area Interconnected Power Systems with Renewable Energy Sources Using Novel PSO~PID-Like Fuzzy Logic Controllers," *Engineering, Technology & Applied Science Research*, vol. 12, no. 3, pp. 8597–8604, Jun. 2022, https://doi.org/10.48084/etasr.4924.

[19] A. Abdennour, "Adaptive Optimal Gain Scheduling for the Load Frequency Control Problem," *Electric Power Components and Systems*, vol. 30, no. 1, pp. 45–56, Jan. 2002, https://doi.org/10.1080/153250002753338391.

[20] H. Yousef, "Adaptive fuzzy logic load frequency control of multi-area power system," *International Journal of Electrical Power & Energy Systems*, vol. 68, pp. 384–395, Jun. 2015, https://doi.org/10.1016/j.ijepes.2014.12.074.

[21] H. A. Yousef, K. AL-Kharusi, M. H. Albadi, and N. Hosseinzadeh, "Load Frequency Control of a Multi-Area Power System: An Adaptive Fuzzy Logic Approach," *IEEE Transactions on Power Systems*, vol. 29, no. 4, pp. 1822–1830, Jul. 2014, https://doi.org/10.1109/TPWRS.2013.2297432.

[22] A. T. Tran *et al.*, "Adaptive Integral Second-Order Sliding Mode Control Design for Load Frequency Control of Large-Scale Power System with Communication Delays," *Complexity*, vol. 2021, no. 1, 2021, Art. no. 5564184, https://doi.org/10.1155/2021/5564184.

[23] K. Liao and Y. Xu, "A Robust Load Frequency Control Scheme for Power Systems Based on Second-Order Sliding Mode and Extended Disturbance Observer," *IEEE Transactions on Industrial Informatics*, vol. 14, no. 7, pp. 3076–3086, Jul. 2018, https://doi.org/10.1109/TII.2017.2771487.

[24] D. Qian, S. Tong, H. Liu, and X. Liu, "Load frequency control by neural-network-based integral sliding mode for nonlinear power systems

with wind turbines," *Neurocomputing*, vol. 173, pp. 875–885, Jan. 2016, https://doi.org/10.1016/j.neucom.2015.08.043.

[25] M. K. Sarkar, A. Dev, P. Asthana, and D. Narzary, "Chattering free robust adaptive integral higher order sliding mode control for load frequency problems in multi-area power systems," *IET Control Theory & Applications*, vol. 12, no. 9, pp. 1216–1227, Jun. 2018, https://doi.org/10.1049/iet-cta.2017.0735.

[26] C. Mu, Y. Tang, and H. He, "Improved Sliding Mode Design for Load Frequency Control of Power System Integrated an Adaptive Learning Strategy," *IEEE Transactions on Industrial Electronics*, vol. 64, no. 8, pp. 6742–6751, Aug. 2017, https://doi.org/10.1109/TIE.2017.2694396.

[27] K. P. S. Parmar, S. Majhi, and D. P. Kothari, "LFC of an interconnected power system with multi-source power generation in deregulated power environment," *International Journal of Electrical Power & Energy Systems*, vol. 57, pp. 277–286, May 2014, https://doi.org/10.1016/j.ijepes.2013.11.058.